

Anisotropic thermal conductivity of nanocolumnar W thin films

Asma Chargui, Raya El Beainou, Alexis Mosset, Joseph Gavaille, Pascal Vairac, Sébastien Euphrasie,

Nicolas Martin ¹

Institut FEMTO-ST, CNRS UMR 6174, Université de Bourgogne Franche-Comté, Besançon, France

Abstract

We report on thermal conductivity of W films 350 nm thick sputter-deposited by glancing angle deposition (GLAD). The 3ω method is used to measure the in-plane thermal conductivity k_x and k_y for films deposited with a deposition angle α of 0° and 80° . For classical films ($\alpha = 0^\circ$), the thermal conductivity is $71 \text{ Wm}^{-1}\text{K}^{-1}$, whereas for GLAD films ($\alpha = 80^\circ$) the in-plane conduction drops to $k_x = 3.2 \text{ Wm}^{-1}\text{K}^{-1}$ and $k_y = 4.8 \text{ Wm}^{-1}\text{K}^{-1}$. The in-plane thermal conductivity anisotropy corresponds to a heat conduction favored in the direction perpendicular to the deposition axis, which is related to the anisotropic columnar microstructure. Electrical conductivity is also determined leading to a significant deviation from the Wiedemann-Franz law for the GLAD films.

Keywords

Glancing Angle Deposition, thermal conductivity, anisotropy, tungsten film

1. Introduction

The GLancing Angle Deposition (GLAD) technique has turned out into an attractive strategy to produce original surface morphologies, especially for designing anisotropic architectures [1]. GLAD films exhibit original physical properties (electrical, thermal, mechanical, and optical behaviors), which are different from the inherent characteristics of the corresponding bulk materials creating new effects [2]. As one of the most interesting physical properties of GLAD films, the thermal conductivity has, until now, been rarely investigated [3]. This gap of knowledge is connected to the difficulty to perform accurate thermal measurements in thin films, which becomes an even more challenging task in porous and nanostructured media like GLAD films. In addition, the rare studies

¹ Corresponding author: nicolas.martin@femto-st.fr

reporting thermal investigations of GLAD films exhibit thermal conductivity lower than a few $\text{Wm}^{-1}\text{K}^{-1}$ for oxide materials mainly [4]. To the best of our knowledge, no studies have been focused on thermal and electrical properties of GLAD metallic thin films.

In this letter, we investigate thermal conductivity and anisotropy of GLAD W films sputter-deposited with 2 deposition angles: $\alpha = 0^\circ$ and 80° . The 3ω experimental technique [5] is used to determine the thermal conductivity of the films, especially the components of the tensor following the two perpendicular in-plane conductivities, namely k_x and k_y . Surface and cross-section microstructures are observed to correlate the porous character and the anisotropic architecture of the W GLAD films with their very low thermal transport behavior. Deviations from the Wiedemann-Franz law are also discussed considering similarly, the in-plane electrical conductivities (σ_x and σ_y) of the films in connection with their inhomogeneous morphological features.

2. Material and Methods

W films were deposited on (100) Si and glass substrates by DC magnetron sputtering in a 40 L homemade chamber at a base pressure below 10^{-5} Pa. More details can be found in the Supplementary Information. Briefly, an argon sputtering pressure of 0.4 Pa was used for all depositions. No external heating was applied during the growth stage, and depositions were carried out at room temperature. The GLAD technique [6] was implemented to produce normal ($\alpha = 0^\circ$) and tilted columnar architectures ($\alpha = 80^\circ$). The deposition time was adjusted to get a constant film thickness of 350 nm. The films morphology (top and cross-section views) was observed by scanning electron microscopy (SEM) with a JEOL JSM 7800 field emission microscope.

The thermal conductivity of the films was measured by the 3ω method [5-7] (to see the Supplementary Information for experimental conditions). A SiO_2 layer (250 – 450 nm thick; acting as an electrical insulator and reducing the air/film roughness) was first deposited on W films by ICPECVD (inductively-coupled plasma chemical vapor deposition). A metallic Pt strip (100 nm thick) was then evaporated and patterned by photolithography and lift-off techniques, acting as heater and sensor. The length of the strips was 3 mm for $\alpha = 0^\circ$ and 1 mm for $\alpha = 80^\circ$, and the width ranging between 2 μm and 30 μm depending on the sample. Strips were either aligned following the x axis (parallel to the particle flux), or the y axis (perpendicular to the particle flux). Isotropic thermal conductivity was calculated for films deposited on Si ($\alpha = 0^\circ$) using the classical method of the up-shift of the in-phase ΔT line according

to the logarithm of the frequency [6]. A sample with the SiO₂ layer but without the W film was assumed as a reference. For samples on glass ($\alpha = 80^\circ$), the model given by Borca-Tasciuc *et al.* [8] based on a two-dimensional heat conduction model was used to extract in-plane thermal conductivities of the films (k_x or k_y depending on the strip orientation). For stripes with the smaller width (2 μm), the contribution of the in-plane conductivities becomes important, i.e., k_y for strips aligned to the x direction (or k_x for y direction). It is also worth noticing that a substrate with a small thermal conductivity (e.g. glass) contributes to the in-plane conductivities. For each sample, the thermal conductivity tensor was extracted from the best fit of doublet for all measurements (different sizes of the strip). The cross-plane thermal conductivity (k_z) was calculated but without meaning and thus not given since it includes unknown values of interface resistances.

Electrical conductivity measurements of W films deposited on glass substrate were performed in air at room temperature. Based-on the van der Pauw configuration (4 probe method), Bierwagen *et al.* [9] proposed an original procedure to determine the in-plane components of the electrical conductivity tensor (and its anisotropy defined as the ratio between electrical conductivity measured following parallel and perpendicular directions to the sputtered particle flux, i.e., σ_x and σ_y , respectively) in the perpendicular directions (x, y) of the films.

3. Results and Discussion

Top and cross-section views by SEM of W films clearly show contrasted morphologies between the two deposition angles (Fig. 1). Conventional sputtered films ($\alpha = 0^\circ$) exhibit a dense microstructure (top view in Fig. 1a) with homogeneous columns perpendicular to the substrate surface (film's thickness and silica layer on top of the film can be seen in Fig. 1c). W films prepared by GLAD ($\alpha = 80^\circ$) display an inclined columnar and nanostructured structure (Fig. 1d). Such sputtering conditions lead to the formation of elongated shaped columns following the direction perpendicular to the incident flux (y direction in Fig. 1b). This morphological asymmetry correlates with the shadowing mechanism and a favored diffusion of the incoming sputtered particles in the direction perpendicular to the incident flux [10]. The column tilt angle β , defined as the angle between the substrate normal and the column center axis, reaches $39 \pm 2^\circ$ for these sputtering conditions. It is worth noting that the deposition of SiO₂ efficiently covers the surface porous microstructure (surface roughness at the film/air interface is reduced) and also ensures an insulating effect.

Thermal conductivity measurements are presented in Table 1. W films sputter-deposited by the conventional sputtering process ($\alpha = 0^\circ$) show no in-plane anisotropy. They exhibit a thermal conductivity of $71 \pm 5 \text{ Wm}^{-1}\text{K}^{-1}$ at room temperature, which is 41% of the W bulk value ($174 \text{ Wm}^{-1}\text{K}^{-1}$). Such a difference between thin films and bulk materials is systematically observed. It is connected to the deposition conditions, the film growth techniques and mainly assigned to structural differences. Micro- to nano-crystalline structures reduce thermal conductivity due to an increased phonon scattering from lattice imperfections, point defects or grain boundaries. In addition, the film/substrate interface has to be considered as a barrier to phonon transport, especially in amorphous or poorly crystallized films.

A substantial drop of thermal conductivity is obtained for W films prepared with $\alpha = 80^\circ$ (column angle $\beta = 39^\circ$) with $k_x = 3.2 \text{ Wm}^{-1}\text{K}^{-1}$ and $k_y = 4.8 \text{ Wm}^{-1}\text{K}^{-1}$ (Table 1). This strong reduction of thermal conductivity is related to the voided architecture, which becomes relevant when the deposition angle α becomes grazing ($\alpha > 70^\circ$). For $\alpha = 80^\circ$, it is commonly reported that the films porosity ratio can be higher than 60% [11], which corresponds to a voided structure and thus, a poor thermal conductive medium, i.e., in the same order of magnitude of polymers or even lower. Imperfections and growing defects are often encountered in GLAD films [12]. Such defects also reduce the thermal conductivity by lowering the effective mean free path of electrons and phonons. In addition, and due to the high porous structure, films are also partially oxidized, lowering their thermal conductivity. It is important to note that interfacial resistances are not assumed in our model, and thus the out-of-plane conductivity k_z is not investigated.

Electrical conduction is similarly influenced by the deposition angle (Table 1). As previously noticed for thermal properties, electrical conductivity of conventional W films ($\alpha = 0^\circ$) is lower than the bulk value due to electron scattering by surfaces and grain boundaries. For both x and y directions, $\sigma_{300\text{K}}$ is close to $7 \times 10^6 \text{ Sm}^{-1}$ (Table 1). Films prepared by GLAD become more resistive and for $\alpha = 80^\circ$, $\sigma_{300\text{K}}$ decreases to $1.7 \times 10^5 \text{ Sm}^{-1}$ for y direction. It is even more reduced following x direction with $\sigma_{300\text{K}} = 8.4 \times 10^4 \text{ Sm}^{-1}$. This drop is mainly assigned to the porosity especially favored by the GLAD process, decreasing the electron mean free path. This porous architecture is particularly marked in the direction of the incident particle flux (x direction) and well correlates with the lowest electrical conductivity. Results in table 1 likewise illustrate the in-plane anisotropy defined as the thermal conductivities ratio ($k_y/k_x = 1.5$ for GLAD W films). The columns cross-section of GLAD W films exhibits an elliptical shape with a major axis following the y direction, which favors the heat flow. Columns tend to chain to each other in this y direction whereas the number

of pathways available following the x direction is reduced due to a more voided medium. Such anisotropic behaviors have similarly been observed for other physical properties like electrical conductivity and surface acoustic waves [13]. These directional-dependent characteristics have systematically been attributed to the fan-like columnar features broadening in the direction orthogonal to the particle flux.

It is worth connecting thermal to electrical conductivity via the Wiedemann-Franz (WF) law, as commonly checked for bulk metals. W films deposited with $\alpha = 0^\circ$ support this law with a Lorenz number L_{300K} of $3.4 \times 10^{-8} \text{ W}\Omega\text{K}^{-2}$ whatever the x or y direction. This value completely agrees with the W bulk value (Table 1). Such a WF law is not well satisfied for GLAD W films since $L_{300K} = 1.3 \times 10^{-7}$ and $9.4 \times 10^{-8} \text{ W}\Omega\text{K}^{-2}$ for x and y directions, respectively. This discrepancy of Lorenz numbers between GLAD and conventional films (and thus bulk) can be assigned to the different effects coming from the free electrons scattering mechanisms (and also to the deposition of SiO_2 layer favoring the W oxidation, especially for GLAD films). Transport properties of electrons serving as charge carriers and heat carriers are scattered by grain boundaries and structural defects, particularly present in GLAD films. Assuming the same probability for electrons to be reflected by such grain boundaries and defects, it leads to different effects on thermal and electrical conductivities and thus, to the violation of the Wiedemann-Franz law [14]. It is also worth noting that the highest Lorenz number is obtained following the x direction. This is directly connected to the elongated pores produced in the direction of the column growth (Fig. 1b). Considering that the thermal conductivity strongly depends on the film morphology and volume fraction of pores, their orientation (orthogonal to the particle flux) mainly impedes heat flow according to the x direction, which leads to a low thermal conductivity.

4. Conclusion

In-plane thermal conductivity of W thin films 350 nm thick was investigated by the 3ω method. Films were sputter-deposited by the GLAD technique using two different deposition angles: $\alpha = 0^\circ$ and 80° . Films with $\alpha = 0^\circ$ showed the expected reduction of the thermal conductivity compared to the bulk, due to the polycrystalline structure of deposited materials. For W GLAD films prepared with $\alpha = 80^\circ$, the thermal conductivity was two orders of magnitude lower than the bulk one. This strong difference was mainly assigned to the voided architecture typically obtained in films prepared by oblique angle deposition at grazing angles ($\alpha > 70^\circ$) and their partial oxidation. A correlation with the electrical conductivity well agrees with the Wiedemann-Franz law for conventional W films ($\alpha = 0^\circ$), whereas a

significant difference was clearly brought to the fore for GLAD W films. This discrepancy was attributed to electrons scattering at grain boundaries and by defects, producing different effects on thermal and electrical behaviors. In addition, oxidation favored by the porous structure and the SiO₂ layer, also contributed to this divergence since W GLAD films becomes reactive towards oxygen and thus deviate from pure metals.

The thermal anisotropy of GLAD W films was finally determined to focus on the in-plane conduction effect. The in-plane anisotropy reached 1.5 due to the elliptical shape of the columns cross-section in the direction perpendicular to the particle flux. This elongated feature of the columns cross-section helps to the heat flow propagation and corroborates other anisotropic behaviors previously reported for electrical conduction and elastic wave propagation.

CRedit authorship contribution statement

Asma Chargui: Writing - Data curation. Raya El Beainou: Data curation. Alexis Mosset: Resources. Joseph Gavaille: Visualization - Review & editing. Pascal Vairac: Supervision. Sébastien Euphrasie: Supervision. Writing - Review & editing. Nicolas Martin: Supervision. Writing - Review & editing.

Declaration of Competing Interest

The authors declare that they have no known competing financial interests or personal relationships that could have appeared to influence the work reported in this paper.

Acknowledgements

This work was supported by the EIPHI Graduate School (contract ANR-17-EURE-0002), the Region of Bourgogne Franche-Comté and the French RENATECH network.

References

- [1] K. Robbie, J. C. Sit, M. J. Brett, Advanced techniques for glancing angle deposition, *J. Vac. Sci. Technol.*, 16 (1988) 1115-1122. <https://doi.org/10.1116/1.590019>
- [2] M.M. Hawkeye, M.T. Taschuk, M.J. Brett. *Glancing Angle Deposition of Thin Films*, John Wiley Sons, Ltd, 2014. <https://doi.org/10.1002/9781118847510>

- [3] J.L. Plawsky, J.K. Kim, E.F. Schubert, Engineered nanoporous and nanostructured films, *Materials Today*, 12 (2009) 36-45. [https://doi.org/10.1016/s1369-7021\(09\)70179-8](https://doi.org/10.1016/s1369-7021(09)70179-8)
- [4] D.D. Hass, A.J. Slifka, H.N.G. Wadley, Low thermal conductivity vapor deposited zirconia microstructures, *Acta Mater.*, 49 (2001) 973-983. [https://doi.org/10.1016/s1359-6454\(00\)00403-1](https://doi.org/10.1016/s1359-6454(00)00403-1)
- [5] D.G. Cahill, Thermal conductivity measurement from 30 to 750 K: The 3ω method, *Rev. Sci. Instrum.*, 61(2) (1990) 802-808. <https://doi.org/10.1063/1.1141498>
- [6] D.G. Cahill, M. Katiyar, J.R. Abelson, Thermal conductivity of a-Si:H thin films, *Phys. Rev. B*, 50 (1994) 6077. <https://doi.org/10.1103/PhysRevB.50.6077>
- [7] M. Bogner, A. Hofer, G. Benstetter, H. Gruber, R.Y.Q. Fu, Differential 3ω method for measuring thermal conductivity of AlN and Si₃N₄ thin films, *Thin Solid Films*, 591 (2015) 267-270. <https://doi.org/10.1016/j.tsf.2015.03.031>
- [8] T. Borca-Tasciuc, A. Kumar, G. Chen, Data reduction in 3ω method for thin-film thermal conductivity determination, *Rev. Sci. Instrum.*, 72 (2001) 2139-2147. <https://doi.org/10.1063/1.1353189>
- [9] O. Bierwagen, R. Pomraenke, S. Eilers, W. T. Masselink, Mobility and carrier density in materials with anisotropic conductivity revealed by van der Pauw measurements, *Phys. Rev. B* 70, (2004) 165307. <https://doi.org/10.1103/physrevb.70.165307>
- [10] A. Chargui *et al.*, Influence of thickness and sputtering pressure on electrical resistivity and elastic wave propagation in oriented columnar tungsten thin films, *Nanomaterials*, 10 (2020) 1-18. <https://doi.org/10.3390/nano10010081>
- [11] T. Ott, G. Gerlach, Morphological characterization and porosity profiles of tantalum glancing-angle-deposited thin films, *J. Sens. Sens. Sys.*, 9 (2020) 79-87. <https://doi.org/10.5194/jsss-9-79-2020>
- [12] R. El Beainou *et al.*, A 4-view imaging to reveal microstructural differences in obliquely sputter-deposited tungsten films, *Mater. Lett.*, 264 (2020) 127381-4. <https://doi.org/10.1016/j.matlet.2020.127381>
- [13] R. El Beainou *et al.*, Electrical conductivity and elastic wave propagation anisotropy in glancing angle deposited tungsten and gold films, *Appl. Surf. Sci.*, 475 (2019) 606-614. <https://doi.org/10.1016/j.apsusc.2019.01.041>

[14] M. Wei-Gang, W. Hai-Dong, Z. Xing, T. Koji, Different effects of grain boundary scattering on charge and heat transport in polycrystalline platinum and gold nanofilm, Chinese Phys. B, 18 (2009) 2035-2040.

<https://doi.org/10.1088/1674-1056/18/5/051>

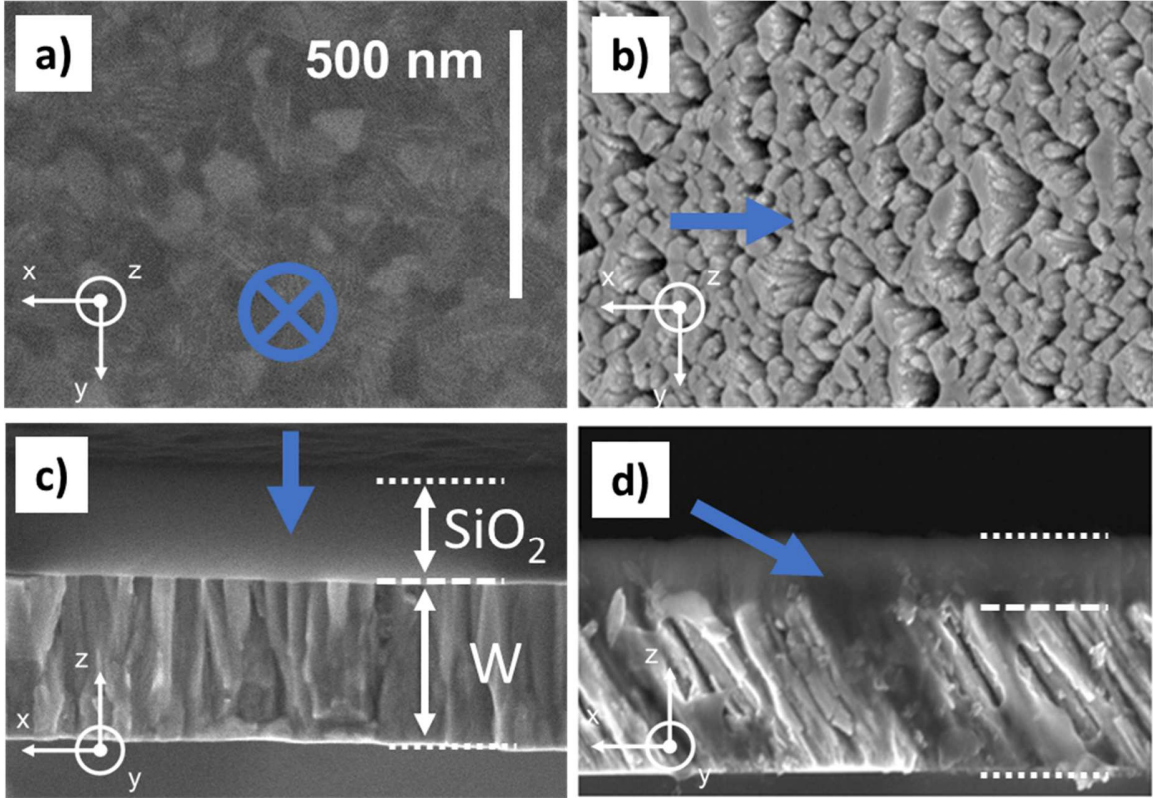


Fig. 1. Top (without SiO₂ layer) and cross-section (with SiO₂ layer) views by SEM of 350 nm thick W thin films sputter-deposited by DC magnetron sputtering: a) and c) with a normal incidence of the particle flux ($\alpha = 0^\circ$); b) and d) with a deposition angle $\alpha = 80^\circ$. The SiO₂ insulating layer is also indicated and the blue arrows show the incoming particle flux. The scale bar is the same for all pictures.

Table 1: Thermal and electrical conductivities following x and y directions, and corresponding Lorenz numbers at 300 K of W thin films 350 nm thick sputter-deposited with deposition angles $\alpha = 0^\circ$ and 80° .

| At 300K | Bulk | $\alpha = 0^\circ$ | $\alpha = 80^\circ$ | |
|---|----------------------|--------------------------------|--------------------------------|--------------------------------|
| Direction | ∇ | ∇ | x | y |
| Electrical conductivity σ_{300K} (Sm ⁻¹) | 1.9×10^7 | $(6.9 \pm 0.1) \times 10^6$ | $(8.4 \pm 0.1) \times 10^4$ | $(1.7 \pm 0.1) \times 10^5$ |
| Thermal conductivity k_{300K} (Wm ⁻¹ K ⁻¹) | 174 | 71 ± 5 | 3.2 ± 0.5 | 4.8 ± 0.5 |
| Lorenz number L_{300K} (W Ω K ⁻²) | 3.1×10^{-8} | $(3.4 \pm 0.3) \times 10^{-8}$ | $(1.3 \pm 0.2) \times 10^{-7}$ | $(9.4 \pm 1.5) \times 10^{-8}$ |